International Journal of Scientific Research and Engineering Development-– Volume 6 Issue 2, Mar-Apr 2023

Available at www.ijsred.com

RESEARCH ARTICLE OPEN ACCESS

Researchon Friction Stir Welding Technique and Electrochemical Corrosion Studies of Dissimilar Aluminium Alloys AA2024 and AA7075

Nithin H M

(Mechanical Department, Rajarajeshwari college of engineering, Banglore

Email: nithingowdahm87@gmail.com)

--************************-----------------------------------

Abstract

The requirement for welding innovation is expanding in the assembling area. FSW is an option in contrast to most of the standard welding processes. The goal of this investigation is to look at the grain size formation and deformation in the welding zone and the speed at which it oxidizes. This study researched the grain development and consumption rate with NaCl arrangement utilizing an EBSD and an SEM assessment. The goal might distinguish any imperfections in FSW and improve the FSW cycle.

Keywords **—FSW, BM, HEZ, SZ, TMAZ**

--************************---------------------------------

I. Introduction

In the future FSW has a wide range of applications due to its welding capabilities. There is a lot of study being done on the FSW method. The FSW of Aluminium is not a new topic, but there is no adequate data available on the welding of dissimilar alloys of Al. Aluminum combinations are broadly utilized in various enterprises because of their low weight, high strength, and protection from consumption. Long-established welding methods like Gas tungsten arc welding (GTAW) and Gas metal arc welding (GMAW) has problems such as porosity, cracking, and distortion when joining aluminium alloys. By combining metals without melting them, friction stir welding (FSW), overcomes these difficulties and produces joints of good mechanical quality. Particularly for connecting aluminium alloys, FSW has attracted a lot of interest recently. The principles of the process, the impact of welding settings on the quality of the joint, and the joint's microstructural and mechanical characteristics. Also, very less is known about welding on both sides of a plate. From this experiment, we will get to know the grain formation in the micro and macro structure of FSW and also the corrosion rate.

II. Friction stir welding technique

Several sectors have had serious concerns about material welding. The welding of comparable materials has historically been the exclusive use of material welding. Due to the quick advancements and need for complicated components in engineering, welding comparable materials has not been able to keep up with industry demands, and researchers' interest in welding dissimilar materials has gradually grown. The Welding Institute (TWI) in the United Kingdom developed FSW as a solid-state joining process in 1991. FSW's rotating welding machine (non-consumable). The foundation plates that must be connected are securely fixed. The tool is gently lowered into the adjacent edges of the plates to be welded while spinning at a constant speed until the tool shoulder contacts the surface of the plates to be welded. The shoulder makes contact with the surface of the workpiece, heating the material. The material to be welded achieves the condition and, by dynamic recrystallization, generates the weld under the impact of rotation, friction, and tool extrusion. The tool shoulder also keeps the material in the weld under control. The apparatus is squeezed toward the weld joint in the wake of preheating. The warming restricts the region encompassing the pin, and the apparatus' interpretation and revolution make material relocate from the front to the back of the device, filling holes in the instrument's way as it advances. As a result, in FSW, frictional heating is used to mechanically attach the components without the need for additional material or stringent requirements.

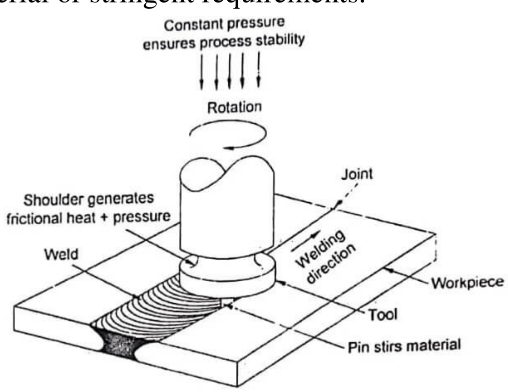

Fig 2The principle of FSW

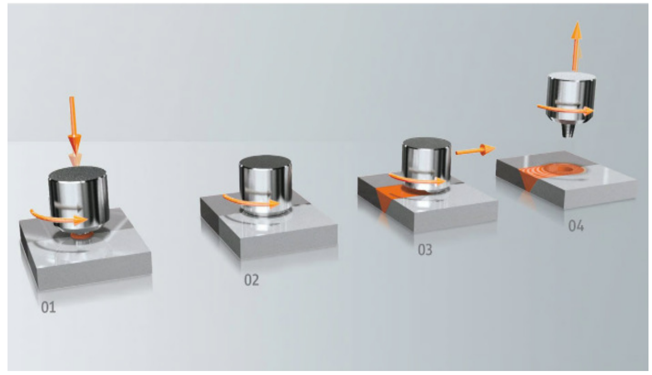

Fig 3Process how FSW is done in 4 different steps

Microstructural Evolution

Various examinations zeroed in on the unmistakable zones shaped during FSW because of extraordinary disfigurement and high temperatures in the Stir zone because of recrystallization. Notwithstanding the way that the mechanical properties are reliant upon grain size due to microstructural heterogeneity, four distinct zones were made. Stir zone (SZ), Thermo-mechanical affected zone (TMAZ), Heat affected zone (HAZ), and Base material (BM) are the

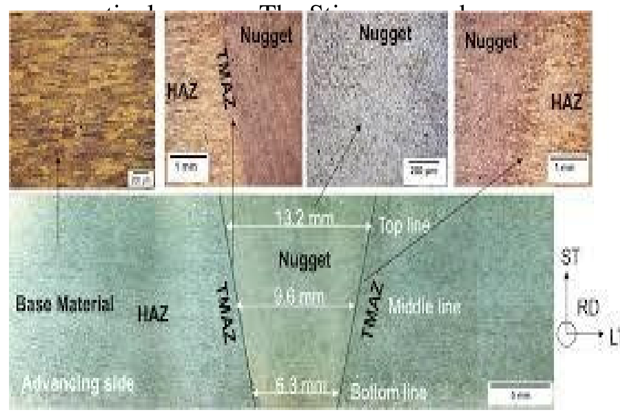

Fig 1 The 4 zones formed from FSW

Fig 4The 4 zones formed from FSW

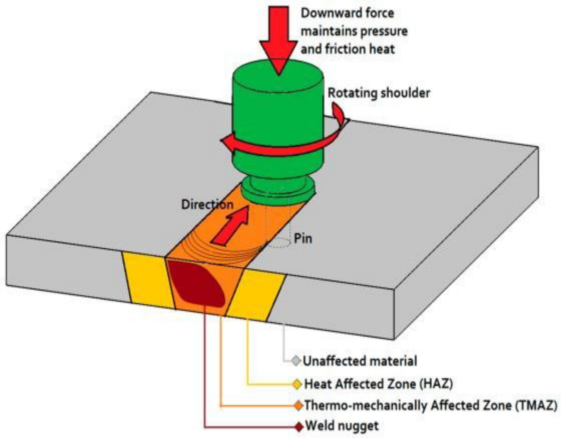

Stir Zone (SZ)

Frictional heat generated by the contact between the rotating tool and the adjacent edges of the work material inside the Stir zone leads to the formation of a recrystallized microstructure with fine-grained materials, commonly referred to as a weld nugget. Stir zones can be found in various shapes and sizes. The Hall-Petch relationship indicates that smaller recrystallization grains exhibit better hardness and strength, while larger grains have inferior mechanical properties. Grain size has a converse relationship with the elasticity and hardness of the material, with a finer grain in the Stir zone indicating the higher mechanical performance of the joint. The recrystallized grain size obtained for underwater FSW is typically smaller than that achieved for FSW in the air due to the lower peak temperature. The size of the recrystallized grains is significantly affected by FSW parameters, tool geometry, the thermal conductivity of the material, workpiece composition, workpiece temperature, and vertical pressure.

Thermo-Mechanically Affected Zone (TMAZ)

Between the heat-affected zone (HAZ) and the Stir zone (SZ) is the Thermo-mechanically affected zone (TMAZ). The grains retain their native microstructure in this location, slightly deformed. Temperature and deformation both have an influence on the TMAZ during FSW. The stir zone on each side has TMAZ regions near it, and a little grain refinement was found in contrast with the base metal. The zone is known as the TMAZ because it is both thermally and precisely affected. Materials in this space hold their unique microstructure however are to some degree contorted during the FSW process, prompting fractional powerful recrystallization. Because of warm mellowing, every one of the joints at the withdrawing sides of the TMAZ has an insignificant hardness. The TMAZ grain size was significantly greater than that of the NZ, and each grain included a lot of precipitates. In a connected report by Khodir and Shibayanagi, it was shown that the precipitation solidifying that was welcomed on by the alloying components maturing normally drove the TMAZ to have a lower hardness than the stir zone however more noteworthy than the HAZ. The TMAZ's lengthened grains are brought about by plastic deformation and the intensity of heat delivered by the FSW tool's stirring motion.

Heat Affected Zone (HAZ)

There is a Heat-affected zone (HAZ) past the TMAZ. This zone needs plastic deformation and solely has thermal effects, making it challenging to change the original grain structure. Contingent upon the condition of the base material and how much dissolve intensity openness, the hardening acceleration in HAZ might harden. In HAZ, Sullivan and Robson found the effect of FSW on the microstructure of the AA7449 aluminum combination, which is 40 mm thick. That's what they guaranteed though grain size doesn't fluctuate in the HAZ, molecule size aspects do, and this change is more articulated as one draws nearer to the TMAZ or SZ. Because of the evacuation of

Guinier-Preston zones and coarsening of reinforcing encouragement, there was a diminishing in microhardness. The FSW process causes precipitates to dissolve, change phases, get coarser, and create a significant precipitate-free zone. According to Jafari's microstructure investigation, the extreme heat input causes the grain size of lower-strength (copper) material at HAZ to grow for higher weld pass numbers.

Base material (BS)

This is the zone that retains its original properties of the material used. Every area beyond the HAZ is the base metal zone. Neither heat nor deformation doesn't play any role here, there is no alteration in the Macrostructure and Microstructure of the material the material remains the same as it was before the welding.

III. A small experiment was conducted on FSW dissimilar aluminium alloys AA2024 and AA7075

Experimental set up

The welding was done at the People's Education Society (PES) university, and about 6 weldings were carried out. The corrosion test was done by Electro Chemical Corrosion Testing Apparatus (Courtesy: East West Institute of Technology, Bengaluru). EBSD and SEM were used to capture the micro and macro structures. Parameters considered for corrosion test were percentages of NaCl (0.035, 0.35 & 3.5) and exposure duration at intervals of 24hrs up to 96hrs at temperatures 27 °C and 40 °C. An Aluminium (AA2024 and AA7075) plate with a thickness of 6mm and length and width (l×w is 100×150 mm) was considered.

For FSW, AA7075 was utilized on the advancing side and in the case of the AA2024 on the retraction side; be that as it may, for double-side welding, the opposite directions were chosen as AA2024 was utilized on the advancing side and AA7075 was used on the retraction side. The fundamental objective was to check whether there were any progressions in the faults formed during welding and root penetration, as well as to look into material fusion caused by welding.

Macrostructure and Microstructure

The macrostructure and microstructure of FSW joints have been thoroughly evaluated so that we may research the quality of a weld joint by evaluating its macrostructure and microstructure also any faults that occur in the future and avoid them in the future. In addition, the grain size and orientation will be investigated.

Macrostructure

The macrostructure of the SZ, HEZ and BM on both single-side welded as well as the double-side welded was captured. The sample is free from welding defects like cracks, porosity and inclusion. No lack of Root penetration was observed & side wall Fusion is complete.

At 400min^{-1}, there is no blending, proposing that no parts have been mixed. Another onion ring type was found in SZ. They are plainly noticeable on the advancing side as opposed to the retracting side and can be seen in both unmistakable and indistinguishable Al alloy of FSW. Accordingly, characterizing the component of onion ring arrangement is challenging. The tool needed to expel a cylindrical-shaped molded material around the device to the retreating side of the joint, then trust that frictional intensity will be produced. Factors like as rotation speed and welding rate can affect the making of onion rings designs. The size of SZ is almost corresponding to the pivot speed because of the rising strain and intensity input up to 1200min^{-1}. This may be on the grounds that higher rotation rates eliminate additional metal cut from the weld zone. These highlights are select to disparate welding joints of Al combinations. Serious macro breaks framed among the metal cut layers on the top surface area of joints between 1600min^{-1} and 2000min^{-1}, turning out to be significantly more extreme when AA2024 amalgam was situated on the withdrawing side. There are no more problems found. Rotation speed and material location are crucial in the formation of distinct Al alloys in FSW joints.

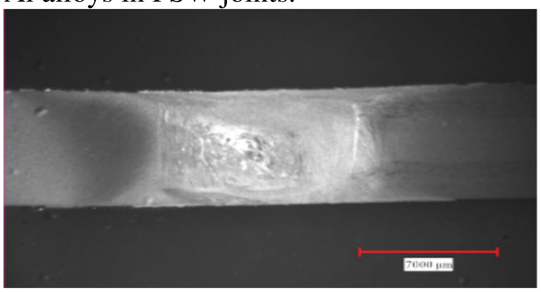

Fig 5 Macrostructure of double side welded zone

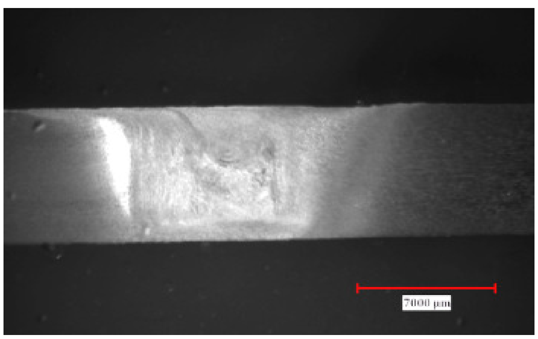

Fig 6Macrostructure of single side welded zone

Microstructure

The microstructure of the BM, HEZ, and SZ on both the single and double-side welded zones was recorded. Many hundred microns long and 40nm broad granules are normal to the weld direction. The alloy generated in the HAZ microstructure on AA7075 alloy is comparable to BM but somewhat darker. The bending angle in the TMAZ is around 70o by the turning welding device, demonstrating the misshapen. In this area, no crystallization happened. When contrasted with BM, the SZ close to 7075 is more modest as opposed to lengthened. The onion ring structure had the option to be consumed by on the other hand rotating dim and rather dim groups. The onion rings that create are laminar, with a fluctuating difference and grain size. There are a few deformities when the 7075 Al compound was on the advancing side which is the reason for the lopsided metal progression of materials because of low temperature.

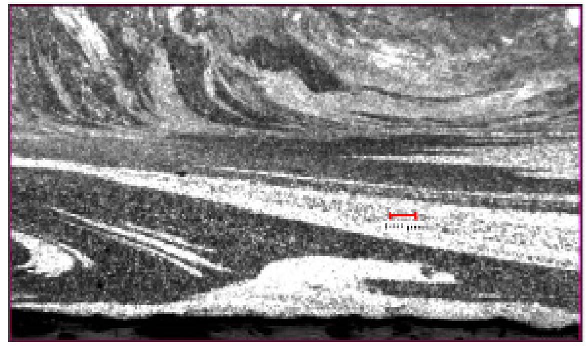

50x Weld

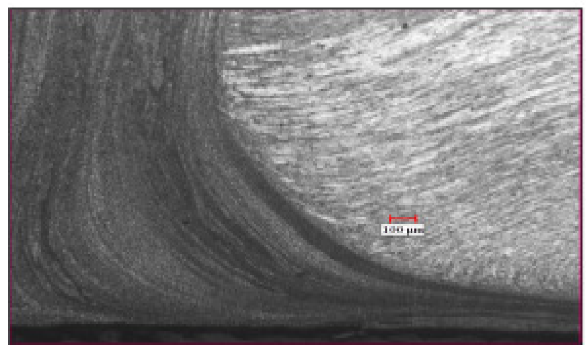

50x HAZ-1

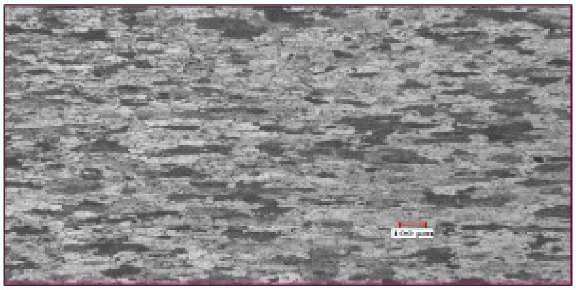

50x Keller's Base

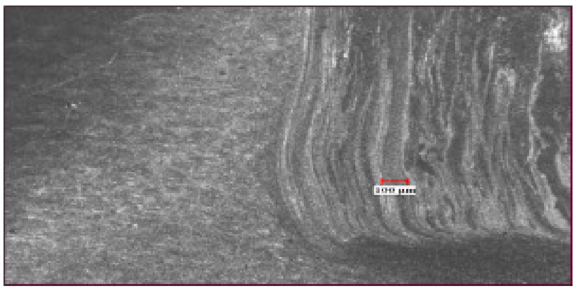

50x HAZ-2

Fig 7Microstructure of a double side welded zone

50x Weld

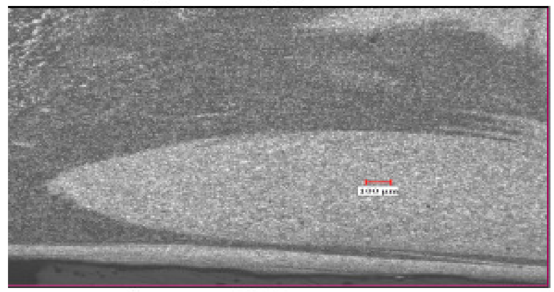

50x HAZ-1

Fig 8Microstructure of a double side welded zone

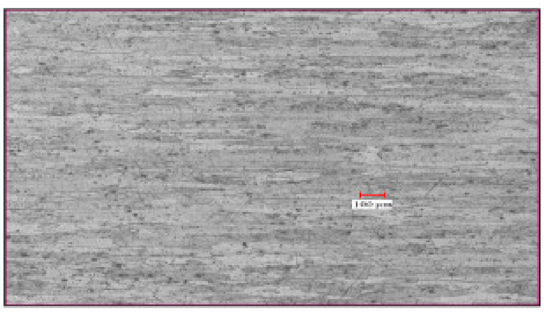

50x base

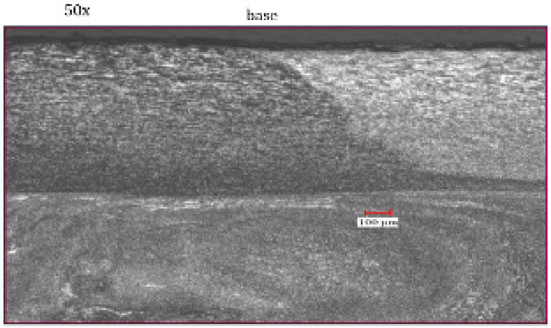

50x HAZ-2

IV. Electron Beam Scattered Microscope (EBSD)

The HAZ, BS and SZ were subjected to Electron Beam Scattered Microscope (EBSD) in a Scanning Electron Microscope (SEM). The ranges of rotation angle from 1^{o} to 5^{o} are marked in red, from 5^{o} to 15^{o} in green and from 15^{o} to 180^{o} is marked in blue. The number obtained in red and blue markings is above 80000 with lengths of 7.33mm & 7.29mm respectively and for green it is around 30000 with a length of 2.75mm.

V. Composition of AA2024 and AA7075

Alloy	Tensile strength	Yield strength	Elongation	Hardness (HBW)	Poisson's Ratio	Thermal conductivity
AA2024	469MPa	324MPa	19%	120	0.33	121W/m-K
AA7075	572MPa	503MPa	11%	150	0.3	130W/m-K

VI. Mechanical Properties of AA2024 and AA7075

Alloy	*Si*	*Fe*	*Cu*	*Mn*	*Mg*	*Cr*	*Zn*	*Ti*	*remaining*
AA2024	*0.07*	*0.2*	*4.23*	*0.52*	*1.17*	*0.01*	*0.15*	*0.05*	*Al*
AA7075	*0.06*	*0.19*	*1.3*	*0.3*	*2.3*	*0.2*	*5.8*	*0.05*	*Al*

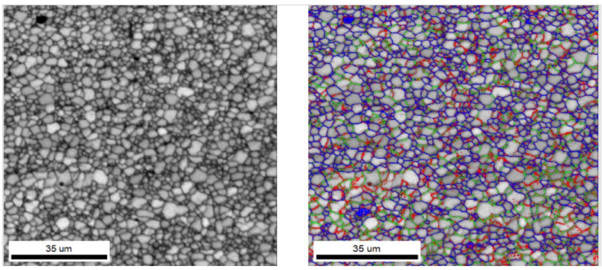

Fig 9SZ- grain size

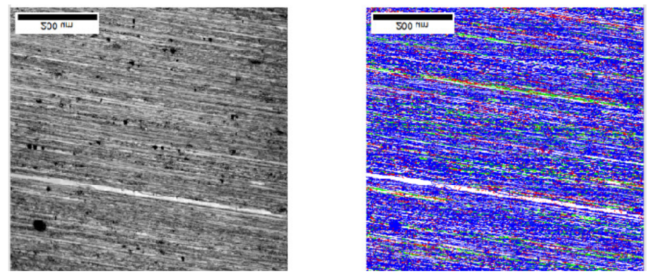

Fig 10HAZ - grain size

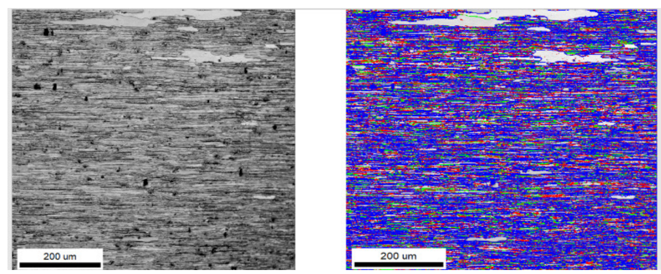

Fig 11BMZ - grain size

Diameter [microns]	Area Fraction
0.2482	0.00111045
0.308144	0.000331343
0.382564	0.000752238
0.474958	0.000996268
0.589666	0.00183582
0.732078	0.0029888
0.908884	0.00691567
1.12839	0.016003
1.40091	0.0264089
1.73925	0.0550298
2.1593	0.101975
2.68079	0.139849
3.32824	0.169218
4.13205	0.144546
5.12999	0.145269
6.36895	0.0867067
7.90712	0.0511276
9.81679	0.0106948
12.1877	0.012591
15.1311	0.02565

Summary Statistics [microns]
Average:
Number 1.93237
Area 4.31351
Standard Deviation:
Number 1.48309
Area 2.88274

SZ

Diameter [microns]	Area Fraction
0.423001	0.000331882
0.549129	0.000104805
0.712865	5.24024e-05
0.925422	0.000221254
1.20136	0.000110627
1.55957	0
2.02459	0
2.62827	0.000483266
3.41196	0
4.42931	0.00146144
5.75001	0.00695787
7.46451	0
9.69023	0.00974102
12.5796	0.0107774
16.3305	0
21.1998	0
27.521	0.209103
35.7271	0
46.38	0.363055
60.2092	0.3976

Summary Statistics [microns]
Average:
Number 6.93264
Area 50.5153
Standard Deviation:
Number 15.036
Area 19.528

HAZ

Diameter [microns]	Area Fraction
1.16093	0.00699908
1.44794	0.00389157
1.80591	0.0126589
2.25238	0.0175511
2.80923	0.0292022
3.50374	0.0355845
4.36996	0.0429653
5.45033	0.0488293
6.79779	0.0589257
8.47838	0.064685
10.5745	0.0697147
13.1887	0.0936378
16.4494	0.113504
20.5161	0.0935157
25.5882	0.114879
31.9142	0.0807819
39.8043	0.0649447
49.6449	0.0120021
61.9185	0
77.2263	0.0357271

Summary Statistics [microns]
Average:
Number 3.87185
Area 18.9561
Standard Deviation:
Number 4.36935
Area 16.15

BM

A1
A2

Gray Scale Map Type:Image Quality
3366.3...12271 (3366.3...12271)

Color Coded Map Type: <none>

Boundaries: Rotation Angle

Min	Max	Fraction	Number	Length
1°	5°	0.422	84687	7.33 mm
5°	15°	0.158	31748	2.75 mm
15°	180°	0.420	84232	7.29 mm

*For statistics - any pair of indexed points with misorientation exceeding 1° or differing in phase is considered a boundary (total number = 200667, total length = 1.74 cm)

The table gives us Grain Size (diameter) which also includes the edge grains in the analysis

VII. Corrosion attack

Zhitong Chen, Shengxi Li, and Lloyd H. Hihara analyzed the mechanical attributes and erosion conduct of the FSW AA5086 and

AA6061 Al compounds. During cathodic polarization in circulated air through 3.15 wt% NaCl, weld zones on the AA6061 side had dispersion-restricted oxygen decrease conduct. FSW AA5086-AA6061 erosion rates for three arrangements were as per the following, from most elevated to least: ASTM seawater > 3.15 weight per cent NaCl > 0.5 M Na2SO4. Following 90 days of submersion, the erosion rate arrived at its most extreme. The consumption pace of 90 days submersion in three arrangements is bigger than that of 120 days drenching in three arrangements because of eroded creation amassing on the outer layer of coupons.

VIII. A corrosion test was conducted to see whether the % of NaCl with respect to different temperature for a time period of around 96hrs effect the rate of corrosion.

The different temperatures considered was 27°C and 40°C, out of which the readings at 40°C were considerable higher compared to that of 27°C. Also, the decrease in NaCl % from 3.5% to 0.035% gave some good corrosion resistance. The rate of corrosion also decreased as long as it was exposed to the NaCl solution.

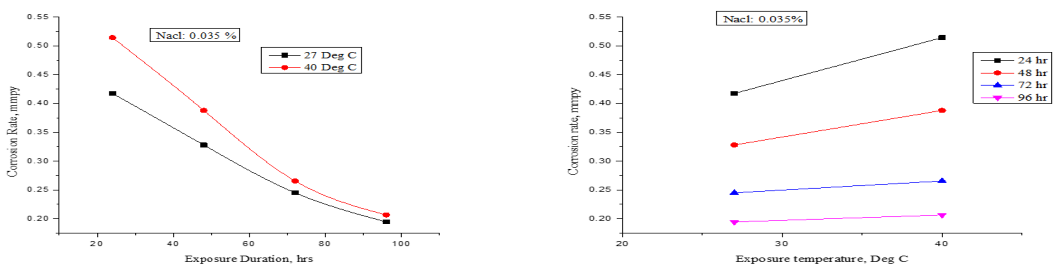

Fig 12Corrosion rates of FSW Aluminium alloy in 0.035 % NaCl solution

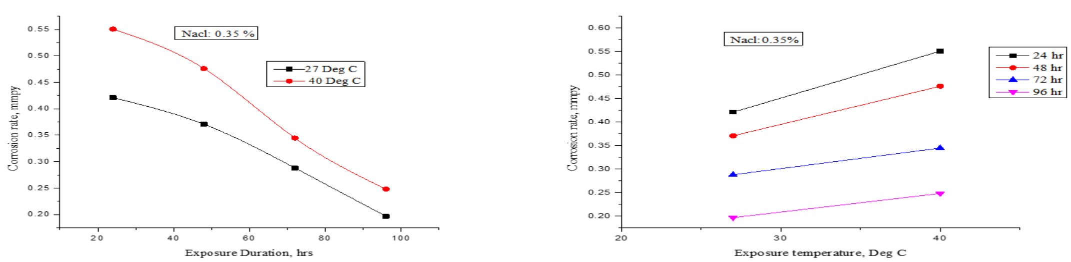

Fig 13Corrosion rates of FSW Aluminium alloy in 0.35 % NaCl solution

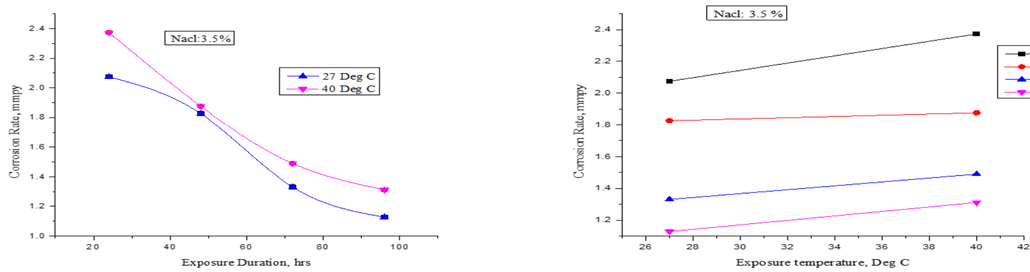

Fig 14Corrosion rates of FSW Aluminium alloy in 3 .5 % NaCl solution

NaCl (%)	**0.035 %**		**0.35 %**		**3.5 %**	
Exposure temperature (°C)	**27**	**40**	**27**	**40**	**27**	**40**
Time in Hour	**Corrosion Rate (mmpy)**					
24	0.4175	0.5143	0.4209	0.5507	2.075	2.373
48	0.3280	0.3881	0.3707	0.4761	1.826	1.876
72	0.2450	0.2655	0.2879	0.3445	1.331	1.490
96	0.1945	0.2066	0.1966	0.2479	1.128	1.312

IX. Results and Discussion

- The corrosion test was coordinated on the FSW Al alloy fluctuating the gathering of sodium chloride solution at different temperatures. The pace of erosion lessens as the length of the time constructs due to the layer plan after the hidden disintegration. The pace of erosion increases at a higher temperature.
- The EBSD results show tremendous microstructural on a micro and macro scale changes during the FSW process, which added to the progression of specific microstructure and restructuring of the grain size in three zones, for instance, ST, TMEZ, and HAZ.
- The microstructural improvement demonstrates that a tremendous piece of the grains through the cross sections experience relative effects inside their genuine region. The grain direction heading addresses the crystallographic lead of the deformed grains during the recrystallization instrument.
- The grain boundary networks at the sub-grain scale have been recognized for the different locale of the weld cross-section, and show different morphology and spatial bearing. The equiaxed grains are attributed to grain division during the welding movement, through the game plan of smaller-than-normal shear bunches across the tremendous grains.
- During the powerful recrystallization process, the interior shear joined with the temperature causes the development of unmistakable more modest grains. In the stir zone, equiaxed fine grains were

framed by recrystallization. In the HAZ, sub-grains were framed and the small portion of the low point grain boundary was expanded because of static recuperation. Grain design and surface parts were kept comparative as contrasted and BM.

X. Applications

Friction mix welding has business involved in different areas, including aviation, marine, auto, and rail transportation. This is a list of the specific applications.

- Aerospace and aviation uses include the production of space shuttle main fuel tanks, rocket launcher core tanks, and fuselage and wing sections. For the A340, A350, and A380 aircraft, FSW was used instead of riveted connections at the wing spar and longitudinal fuselage skin. Friction mix welding is likewise utilized in the development of the floorboards of the tactical Airbus A400M.

- Subway and rail car component welding is an essential feature of the rail transportation business. The marine and street transportation area incorporates spans, decks, bodies, and inside structures for fast ships.

- The iMac, Apple's most well-known work area model, as of late utilized FSW to associate the particles of two aluminium surfaces, bringing about a smooth, exact, and particularly impressive intersection. This helped the organization in diminishing the heaviness of the work area by around 40%.

- Aluminium alloys AA5083 were used in the tube, and AA6063 was utilised in the front and rear axle bodies. This is a feature of BMW Model 5 cars. The inside of the ship is composed of AA6063 aluminium alloy, and the hulls are made of AA5083.

- To make engine cradles, Honda Corporation employed multiple lap joints made of iron and aluminium. These two compounds have been employed in storage tanks, cooking appliances, and a variety of industrial applications (St-52 and AA5005). Furthermore, the door panels were made of steel and aluminium alloys to reduce vehicle weight while boosting fuel efficiency and other dynamic characteristics.

- Additional applications for uncommon high-strength material combinations include SS (stainless steel) and Ni-based superalloys.

References

1. Yunus, Mohammed, and Turki Alamro. "Evaluation of wear and corrosion properties of FSWed aluminium alloy plates of AA2020-T4 with heat treatment under different aging periods." *Reviews on Advanced Materials Science* 61.1 (2022): 687-697.
2. Leon, J. Stephen, G. Bharathiraja, and V. Jayakumar. "A review on friction stir welding in aluminium alloys." *IOP conference series: materials science and engineering*. Vol. 954. No. 1. IOP Publishing, 2020.

3. Shah, Pratik H., and Vishvesh J. Badheka. "Friction stir welding of aluminium alloys: an overview of experimental findings–process, variables, development and applications." *Proceedings of the Institution of Mechanical Engineers, Part L: Journal of Materials: Design and Applications* 233.6 (2019): 1191-1226.
4. Reddy, N. Ravinder, and G. Mohan Reddy. "Friction stir welding of aluminium alloys-a review." *International Journal of Mechanical Engineering and Technology* 7.2 (2016): 83-90.
5. ShivaKumar, G. N., and G. Rajamurugan. "Friction stir welding of dissimilar alloy combinations—A Review." *Proceedings of the Institution of Mechanical Engineers, Part C: Journal of Mechanical Engineering Science* 236.12 (2022): 6688-6705.
6. Chen, Zhitong, Shengxi Li, and Lloyd H. Hihara. "Electrochemical and mechanical behaviors of dissimilar friction stir welding between 5086 and 6061 aluminium alloy." *arXiv preprint arXiv:1802.03460* (2018).
7. Salih, Omar S., et al. "A review of friction stir welding of aluminium matrix composites." *Materials & Design* 86 (2015): 61-71.
8. Tiwari, S. K., Dinesh Kumar Shukla, and R. Chandra. "Friction stir welding of aluminium alloys: a review." *International Journal of Materials and Metallurgical Engineering* 7.12 (2013): 2403-2408.
9. Zhang, Chenghang, Guangjie Huang, and Qing Liu. "Quantitative analysis of grain structure and texture evolution of dissimilar AA2024/7075 joints manufactured by friction stir welding." *Materials Today Communications* 26 (2021): 101920.
10. Zhang, Chenghang, et al. "Microstructure evolution of thermo-mechanically affected zone in dissimilar AA2024/7075 joint produced by friction stir welding." *Vacuum* 179 (2020): 109515.
11. Zhang, Chenghang, et al. "Investigation on microstructure and localized corrosion behaviour in the stir zone of dissimilar friction-stir-welded AA2024/7075 joint." *Journal of Materials Science* 55 (2020): 15005-15032.
12. Khodir, Saad Ahmed, and Toshiya Shibayanagi. "Microstructure and mechanical properties of friction stir welded dissimilar aluminium joints of AA2024-T3 and AA7075-T6." *Materials transactions* 48.7 (2007): 1928-1937.
13. Zhang, Chenghang, et al. "Optimization of tensile and corrosion properties of dissimilar friction stir welded AA2024-7075 joints." *Journal of Materials Engineering and Performance* 28 (2019): 183-199.
14. Çam, G. and M. Koçak, *Progress in joining of advanced materials.* InternationalMaterialsReviews,1998. **43**(1): p.1-44.
15. Hassan, A.M., M. Almomani, T. Qasim, and A. Ghaithan, *Effect of ProcessingParametersonFrictionStirWeldedAluminiumMatrixCompositesWearBehavior.*MaterialsandManufacturingProcesses,2012.**27**(12):p.1419-1423.
16. Suryanarayanan, K., R. Praveen, and S. Raghuraman, *Silicon Carbide ReinforcedAluminium Metal Matrix Composites for Aerospace Applications: A LiteratureReview.* International Journal of Innovative Research in Science Engineering andTechnology, 2013.**2**(11).
17. Ellis, M.B.D., *Joining of aluminium based metal matrix composites.* InternationalMaterialsReviews,1996. **41**(2): p.41-58.
18. Huang, R.Y., S.C. Chen, and J.C. Huang, *Electron and laser beam welding of*

highstrain rate superplastic Al-6061/SiC composites. Metallurgical and MaterialsTransactions a-Physical Metallurgy and Materials Science, 2001. **32**(10): p. 2575-2584.

19. Thomas, W., E. Nicholas, J. Needham, M. Murch, P. Temple-Smith, and C. Dawes,*Friction Stir Butt Welding, International Patent No. PCT/GB92/02203, GB PatentNo. 9125978.8,1991,U.S.Patent No.5,460,317,1995*.1991.
20. *Metal Matrix Composites (MMC) Market for Ground Transportation,Electronics/Thermal Management, Aerospace and Other End-users - GlobalIndustry Analysis, Size, Share, Growth, Trends and Forecast, 2013 - 2019*. 2014[cited 2015; Available from: https://www.linkedin.com/pulse/20140605070839-173774513-metal-matrix-composites-market-review.
21. Kaczmar, J., K. Pietrzak, and W. Włosiński, *The production and application ofmetal matrix composite materials.* Journal of Materials Processing Technology,2000.**106**(1): p.58-67.
22. P.Cavaliere,A.Squillace,andF.Panella,"Effectofweldingparametersonmechanicaland microstructuralpropertiesofAA6082joints produced by friction stir welding," *Journal of Materials ProcessingTechnology*,vol.200,pp.364-372,2008.
23. P. Cavaliere, G. Campanile, F. Panella, and A. Squillace, "Effect ofwelding parameters on mechanical and microstructural properties ofAA6056 joints produced by friction stir welding," *Journal of MaterialsProcessingTechnology*,vol.180,pp.263-270,2006.
24. P. Cavaliere, D. A. Santis, F. Panella, and A. Squillace, "Effect ofanisotropy on fatigue properties of 2198 Al-Li plates joined by frictionstirwelding,"*EngineeringFailureAnalysis*, vol. 6,pp. 1856-1865,2008.
25. P. Cavaliere, D. A. Santis, F. Panella, and A. Squillace, "Effect ofwelding parameters on mechanical and microstructural properties ofdissimilar AA6082-AA2024 joints produced by friction stir welding,"*MaterialsandDesign*,vol.30,pp.609-616,2009.
26. P. Cavaliere, R. Nobile, F. W. Panella, and A. Squillace, "Mechanicaland microstructural behaviour of 2024-7075 aluminium alloy sheetsjoined by friction stir welding," *International Journal of Machine Tools&Manufacture*,vol.46,pp.588-594,2006.
27. H. Aydin, A. Bayram, A. Uguz, and S. K. Akay, "Tensile properties offriction stir welded joints of 2024 aluminium alloys in different heat-treated-state,"*MaterialsandDesign*,vol.30,pp.2211-2221,2009.
28. W.Xu,J.Liu,G.Luan,andC.Dong,"Temperatureevolution,microstructure and mechanical properties of friction stir welded thick2219-O aluminium alloy joints,"*Materials and Design*, vol. 30, pp.3460-3467,2008.
29. O.Hatamleh,"Acomprehensiveinvestigationontheeffectsoflaserandshot peening on fatigue crack growth in friction stir welded AA 2195joints,"*InternationalJournalofFatigue*,vol.31,pp.974-988,2009.
30. O. Hatamleh, and A. DeWald, "An investigation of peening effects onthe residual stresses in friction stir welded

2195 and 7075 aluminiumalloy joints," *Journal of Materials Processing Technology*, vol. 209, no.10,pp.4822-4829,2009.
31. W.Xu,J.Liu,G.Luan,andC.Dong,"Temperatureevolution,microstructure and mechanical properties of friction stir welded thick2219-O aluminium alloy joints,"*Materials and Design*, vol. 30, pp.3460-3467,2008.
32. H. Aydin, A. Bayram, and I. Durgun, "The effect of post-weld heattreatment on the mechanical properties of 2024-T4 friction stir-weldedjoints,"*MaterialsandDesign*,vol.31, pp.2568-2577,2010.
33. M. A.Sutton, B.Yang,A. P.Reynolds and J.Yan:Mater.Sci. Eng. A 364(2004)66–74.
34. W.XunhongaandW.Kuaishe:Mater.Sci.Eng. A431(2006)114–117.
35. C.G.Rhodes,M.W.Mahoney,W.H.Bingel,R.A.SpurlingandC.C.Bampton:ScriptaMaterialia36(1997)69–75.
36. H.S.Park,T.Kimura,T.Murakami,Y.Nagano, K.NakataandM.Ushio:Mater.Sci.Eng.A371(2004)160–169.
37. H.Fujii,L.Cui,N.Tsuji,M.Maeda,K.NakataandK.Nogi:Mater.Sci.Eng.A429(2006)50–57.
38. Y.S.Sato,T.W.Nelson,C.J.Sterling,R.J.Steel andC.-O.Pettersson:Mater.Sci.Eng.A397(2005)376–384.
39. C.J.DawesandW.M.Thomas:Weld.J.75(1996)41–45.
40. R. Zettle, S. Lomolino, J. Dossantos, T. Donath, F. Beckmann, T.LippmanandD.Lohwasser:*ProceedingofIIWPre-AssemblyMeetingonFSW*(Nagoya,Japan,2004)65–70.
41. R.S.MishraandZ.Y.Ma:Mater.Sci.Eng.R50(2005)1–78.
42. A.Steuwer,M.J.PeelandP.J.Withers:Mater.Sci.Eng.A441(2006) 187–169.
43. J.Ouyang,E.YarrapareddyandR.Kovacevic: J.Mater.Process.Technol.172(2006)110–122.
44. J.Yan,Z.Xu,Z.Li,L.LiandS.Yang:ScriptaMaterialia53(2005)585–589.
45. L.CederqvistandA.P.Reynolds:Weld.J.80(2001)281–287.
46. P.Cavaliere,R.Nobile,F.W.PanellaandA.Squillace:Inter.J.ofMachineTools&Manufact. 46(2006)588–594.
47. K.N.Krishnan:Mater.Sci.Eng.A327(2002)246–251.
48. P.L.Threadgill:Stateoftheart,TWIreport(1999)678.
49. S.A.Khodir,T.ShibayanagiandM.Naka:Mater.Trans.47(2006)185–193.
50. P.B.Srinivasan,W.Dietzel,R.Zettler,J.F.DosSantosandV.Sivan:Mater.Sci.Eng.A392(2005)292–300.
51. Y.Li,L.E.MurrandJ.C.McClure:ScriptaMaterialia40(1999)1041–1046.
52. W.B.Lee,Y.M.YeonandS.B.Jung:ScriptaMaterialia49(2003)423–428.
53. C.Genevois,A.Deschamps,A.DenquinandB.Doisneau-cottignies:ActaMater.53(2005)2447–2458.
54. T.Venugopal,K.SrinivasaRaoandK.Prasad Rao:Trans.Indian.Inst.Met57(2004)659–663.
55. M.J.Jones,P.Heurtier,C.Desrayaud,F.Montheillet,D.Allehaux and J.H.Driver:ScriptaMaterialia52(2005)693–697.

